

# FORTGESCHRITTENEN-PRAKTIKUM II

---

## Muon decay

---

April 20 to 24, 2015

Moritz  
BITTERLING

Benjamin  
ROTTLER

Supervisor: Manfredi RONZANI



INSTITUT FÜR MATHEMATIK UND PHYSIK  
ALBERT-LUDWIGS-UNIVERSITÄT  
FREIBURG IM BREISGAU

All calculations and plots in this protocol were done with Python 3.4 using the following libraries

- PyROOT (<http://root.cern.ch/drupal/content/pyroot>)
- NumPy (<http://www.numpy.org/>)

All graphics were drawn with Inkscape (<http://www.inkscape.org>)

The python-scripts, L<sup>A</sup>T<sub>E</sub>X-scripts and svg-graphics can be accessed online under <https://github.com/Bigben37/FP2/tree/master/0420-Myon>.

# Contents

<b>1. Aim of the experiment</b>	<b>1</b>
<b>2. Physical principles</b>	<b>1</b>
2.1. Standard Model . . . . .	1
2.2. The muon . . . . .	2
2.3. Energy loss via ionization and excitation . . . . .	4
2.4. (V-A)-theory . . . . .	5
2.5. Scintillators . . . . .	6
2.6. Photomultipliers . . . . .	6
<b>3. Experimental setup</b>	<b>7</b>
<b>4. Experimental procedure</b>	<b>15</b>
4.1. Energy resolution: Photoelectronstatistics . . . . .	15
4.2. Energy calibration . . . . .	16
4.3. Time calibration . . . . .	17
4.4. Underground measurement . . . . .	17
4.5. The $\beta$ -spectrum and the mean lifetime . . . . .	18
4.6. Schedule of the experiment . . . . .	18
<b>5. Measurement results and evaluation</b>	<b>19</b>
5.1. General remarks . . . . .	19
5.2. Energy resolution . . . . .	19
5.3. Energy calibration . . . . .	22
5.4. Time calibration . . . . .	27
5.5. Underground . . . . .	29
5.6. $\beta$ -spectrum . . . . .	30
5.7. Mean lifetime . . . . .	32
5.8. Weak coupling constant . . . . .	33
<b>A. Appendix</b>	<b>34</b>
A.1. Lab report . . . . .	34

## 1. Aim of the experiment

In the experiment a component of cosmic radiation is investigated: Muons which are produced in the atmosphere are detected in a tank filled with a liquid scintillator. Measurements of mass and lifetime of muons will be realised. A major component of the experiment is the set-up and adjustment of the analyzing equipment and the conduction of various calibrations. The results of the measurements will be used to calculate the coupling constant of the weak interaction.

## 2. Physical principles

### 2.1. Standard Model

The *Standard Model of particle physics* describes all known elementary particles (Figure 2.1) and the different interactions between them.

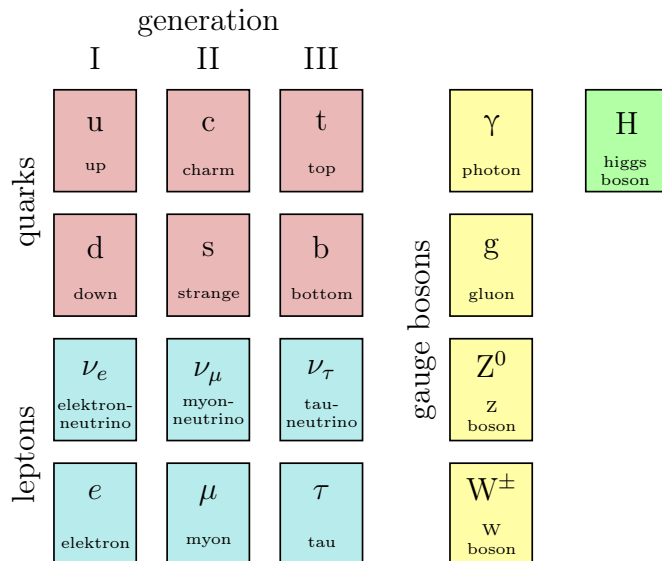


**Figure 2.1:** The known particles of the Standard Model.

The four known interactions are gravitation, electromagnetism, strong and weak interaction. Not all elementary particles obey all interactions.

Elementary particles are the smallest particles currently known, until now there was no substructure found. This doesn't mean that they are stable or free observable. They divide into fermions (spin  $\frac{1}{2}$ ) that make up matter and gauge bosons (spin 1), listed in Table 2.1, which carry the fundamental interactions. Furthermore there is the Higgs boson, which is not a direct result of a gauge theory and therefore doesn't carry a fundamental force. But it is needed to combine the electromagnetic and weak interactions and to give the Z- and W-bosons their mass.

Fermions can be divided into six quarks, which interact via the strong interaction, and

**Table 2.1:** Gauge bosons and their interaction.

gauge boson	interaction
photon ( $\gamma$ )	electromagnetic
gluon (g)	strong
Z-boson ( $Z^0$ )	weak
W-boson ( $W^\pm$ )	weak

six leptons, which don't. Both quarks and fermions are divided into three generations, each with two particles. Equivalent particles of those generations have almost the same properties except for their mass.

## 2.2. The muon

Muons are charged ( $z = \pm 1$ ) leptons of the second generation. They have a mass<sup>1</sup> of

$$E_\mu = (105.6583715 \pm 0.0000035) \text{ MeV} \quad (2.1)$$

and a mean lifetime<sup>2</sup> of

$$\tau_\mu = (2.1969811 \pm 0.0000022) \mu\text{s} . \quad (2.2)$$

### 2.2.1. Muon decay

Muons decay into electrons or positrons (Figure 2.2):

$$\mu^- \rightarrow e^- + \nu_\mu + \bar{\nu}_e \quad \mu^+ \rightarrow e^+ + \bar{\nu}_\mu + \nu_e \quad (2.3)$$

This is a three body decay, the energy spectrum corresponds to normal  $\beta$ -decay spectrum.

The time dependency of a decaying sample of muons can be described with the normal exponential decay law:

$$\frac{dN}{dt} = -\lambda N \quad \Rightarrow \quad N(t) \propto e^{-\lambda t} \quad (2.4)$$

where  $N$  is the number of particles and  $\lambda$  the exponential decay constant. The mean lifetime calculates to:

$$\tau := \frac{\langle t \rangle}{\int_0^\infty N(t) dt} = \frac{\int_0^\infty t e^{-\lambda t} dt}{\int_0^\infty e^{-\lambda t} dt} = \frac{\frac{1}{\lambda^2}}{\frac{1}{\lambda}} = \frac{1}{\lambda} \quad (2.5)$$

After this time only  $\frac{1}{e} \approx 37\%$  of an initial amount of muons exist. The mean lifetime applies to the rest frame of the muon.

---

<sup>1</sup>[http://physics.nist.gov/cgi-bin/cuu/Value?mmuc2mev|search\\_for=muon](http://physics.nist.gov/cgi-bin/cuu/Value?mmuc2mev|search_for=muon) (visited May 9, 2015)

<sup>2</sup>J. Beringer *et al.* (Particle Data Group), PR **D86**, 010001 (2012) and 2013 partial update for the 2014 edition

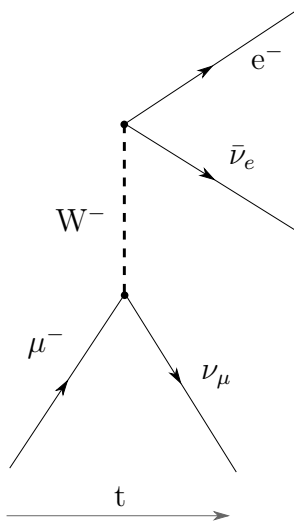


**Figure 2.2:**  $\mu^-$  decay into  $e^-$ ,  $\nu_\mu$  and  $\bar{\nu}_e$ .

### 2.2.2. Origin of muons

The information in this section is based on [1] and [3].

Muons are produced by cosmic rays in the earth's atmosphere. There are two different kinds of radiations, the primary radiation and the secondary radiation.

**Primary radiation** The origin of primary radiation is not clear, but there are assumptions that the particles originate from supernovae and pulsars. Protons make the largest component of primary radiation with 92%. Furthermore it consists of helium cores ( $\alpha$ -particles) with a percentage of 7% and electrons with 1%. Heavy cores are rarely measured. The energy spectrum ranges from  $10^7$  eV to  $10^{20}$  eV, whereas particles with less energy are more common.

**Secondary radiation** While entering the atmosphere primary particles collide with the atoms of the atmosphere. A variety of generation and annihilation processes occur. This happens usually in a height of 15-20 km. Important for this experiment is the generation of pions and kaons:

$$p + \text{nucleus} \rightarrow \pi^{0,\pm}, K^{0,\pm}, n, p \quad (2.6)$$

The charged pions and kaons decay after a short time, some into muons:

$$\begin{aligned} \pi^+ &\rightarrow \mu^+ + \nu_\mu \\ \pi^- &\rightarrow \mu^- + \bar{\nu}_\mu \\ K^+ &\rightarrow \mu^+ + \nu_\mu \\ K^- &\rightarrow \mu^- + \bar{\nu}_\mu \end{aligned} \quad (2.7)$$

There are more positive muons than negative ones, this is caused by two reasons: It is far more probable that a proton, which has a positive charge, generates also a positive

particle by interaction with the atoms of the atmosphere. Furthermore, like electron capture, negative muons can be caught by a nucleus.

### 2.2.3. Relativistic muons

With classical physics one would not expect the muons to reach the ground. With a mean lifetime of approximately  $\tau = 2.2\text{ }\mu\text{s}$  they would travel with a velocity close to light speed only a distance of  $\tau c = 660\text{ m}$ . The reason why muons can be detected anyhow is special relativity. Muons generated by cosmic rays have such a high energy that their mean lifetime observed from earth increases by a factor<sup>3</sup> of  $\gamma$  because of time dilation. For example: A muon with  $E = 10.5\text{ GeV}$  has a observed mean lifetime of  $\tau' = \gamma\tau = 218.6\text{ }\mu\text{s}$  and travels  $65.6\text{ km}$  on average.

Now one can also calculate the percentage  $\frac{N}{N_0}$  of muons ( $E = 10.5\text{ GeV}$ ) which reach the ground with [Equation 2.4](#):

$$\frac{N}{N_0} = e^{-\frac{t}{\tau'}} = e^{-\frac{s}{v\tau'}} \quad (2.8)$$

With  $s = 15\text{ km}$  and  $v \approx c$  the calculation yields  $\frac{N}{N_0} = 79.6\%$ .

## 2.3. Energy loss via ionization and excitation

When particles interact with matter they can lose energy via elastic collisions or through excitation or ionization of the electrons in the atomic shell. This effect is used to detect particles, for example it is utilized by the scintillators in this experiment. The average energy loss per path length  $-\frac{dE}{dx}$  can be calculated using the *Bethe formula*. The following formula applies to relativistic particles ([2], p. 87-89, formula slightly remodeled):

$$-\frac{dE}{dx} = \frac{4\pi}{m_e c^2} \cdot \frac{n_e z^2}{\beta^2} \cdot \left( \frac{e^2}{4\pi\epsilon_0} \right)^2 \cdot \left[ \ln \left( \frac{2m_e c^2 \beta^2}{E_b (1 - \beta^2)} \right) - \beta^2 \right] \quad (2.9)$$

Nomenclature:

- detector: electron density  $n_e$ , mean binding energy of electrons  $E_b$
- particle: charge number  $z$ , ratio of velocity to the speed of light  $\beta = \frac{v}{c}$
- constants: mass of electron  $m_e$ , vacuum permittivity  $\epsilon_0$ , speed of light  $c$

Two notable dependencies of  $-\frac{dE}{dx}$  are the quadratic one on the charge,  $-\frac{dE}{dx} \sim z^2$  and the inverse quadratic one on the relative velocity,  $-\frac{dE}{dx} \sim \frac{1}{\beta^2}$ . There is no dependency on the mass of the incidental particle.

The qualitative graph of the *Bethe formula* is shown in [Figure 2.3](#).

---

<sup>3</sup>The Lorentz factor. Here  $\gamma$  can be calculated with  $\gamma = \frac{E}{E_0}$ , where  $E$  is the energy and  $E_0$  the rest energy of the muon.

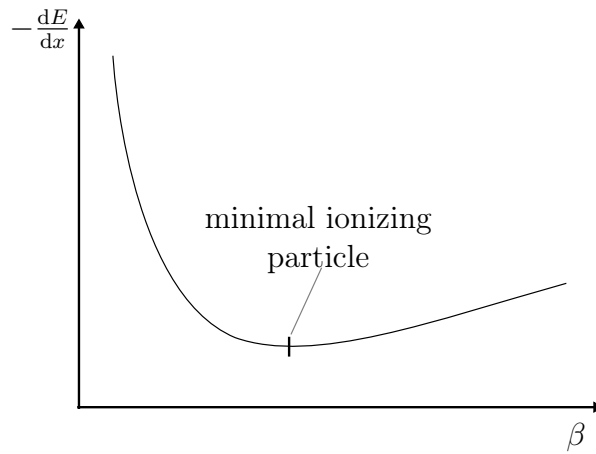


**Figure 2.3:** Bethe formula: Average energy loss per path length  $-\frac{dE}{dx}$  of a particle with relative velocity  $\beta$ .

For small values of  $\beta$  the graph behaves like  $\sim \frac{1}{\beta^2}$ , for large values like  $\sim \ln\left(\frac{\beta^2}{1-\beta^2}\right)$ . In between there is a minimum, those particles with the minimal energy loss per length are called *minimal ionizing particles*.

## 2.4. (V-A)-theory

The (V-A)-theory<sup>4</sup> is a model for the weak interaction based on Fermi's theory of weak interaction. Today it is used as a low energy approximation for the latest theory. Since the theory is quite complicated and is not in the curriculum of a bachelor's degree a reference for the calculation of the muon decay is made to [3] (p. 19-23). The formula for the mean lifetime  $\tau_\mu$  of a muon is

$$\tau_\mu = \frac{192\pi^3\hbar^7}{G_\mu^2 m_\mu^5 c^4} . \quad (2.10)$$

If the mass  $m_\mu$  and the mean lifetime  $\tau_\mu$  of the muon is known, the weak coupling constant  $G_\mu$  can be calculated:

$$G_\mu = \sqrt{\frac{192\pi^3\hbar^7}{\tau_\mu m_\mu^5 c^4}} \quad (2.11)$$

The literature value<sup>5</sup> is:

$$G_\mu = (1.166364 \pm 0.000005) \cdot 10^{-5} \frac{1}{\text{GeV}^2} \quad (2.12)$$

<sup>4</sup>vector-axialvector

<sup>5</sup><http://physics.nist.gov/cgi-bin/cuu/Value?gf> (visited May 9, 2015)

## 2.5. Scintillators

Muons can be detected using scintillating materials. Here a short introduction to the mechanism of scintillation will be given (the information is according to [2] and [3]). In scintillators the interaction of high-energy particles and matter is used to determine the energy of the particle: As it passes through the scintillating material, it excites electrons. The excitation energy amounts to several electronvolts and the number of excited electrons is (in the ideal case of complete absorption) proportional to the energy of the particle. To be able to measure the ultraviolet light that is emitted when the electrons fall back into their ground state, the scintillator has to be transparent for light of this wavelength. This is achieved using a wavelength shifter, a substance that exhibits a large *stokes shift*: If an electron in the ground state is excited, it enters a higher energy level. Additionally, vibrational states of the molecule are excited. A small amount of energy is emitted promptly through vibrational relaxation, so the energy of the photon that is produced when the electron falls back in the ground state is smaller than the absorbed photon (stokes shift). For the emitted photon, the scintillator is transparent, thus it can exit and be detected by a photomultiplier.

## 2.6. Photomultipliers

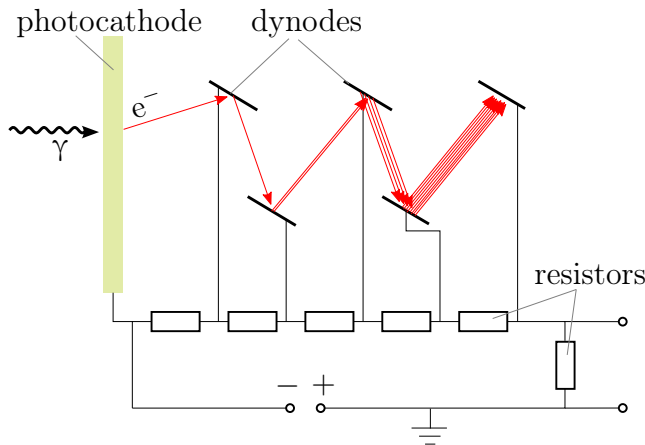


**Figure 2.4:** Composition of a photomultiplier for the transduction of weak light signals into current pulses.

The light signal delivered by a scintillating material is very faint, thus it needs intensification. Photomultipliers are used for this task.

In a photomultiplier, photons hit a photocathode and create free electrons by reason of the photoeffect. The electrons are accelerated in an electric field to the first dynode of the photomultiplier (Figure 2.4). The following dynodes are connected to a voltage divider in a way that the next dynode has a more positive potential. Thereby the avalanche of electrons that is provoked by a few photons is amplified: An electron that hits a dynode generates several free electrons. This effect produces an output signal at the end of the photomultiplier whose intensity is proportional to the number of incoming photons.

### 3. Experimental setup

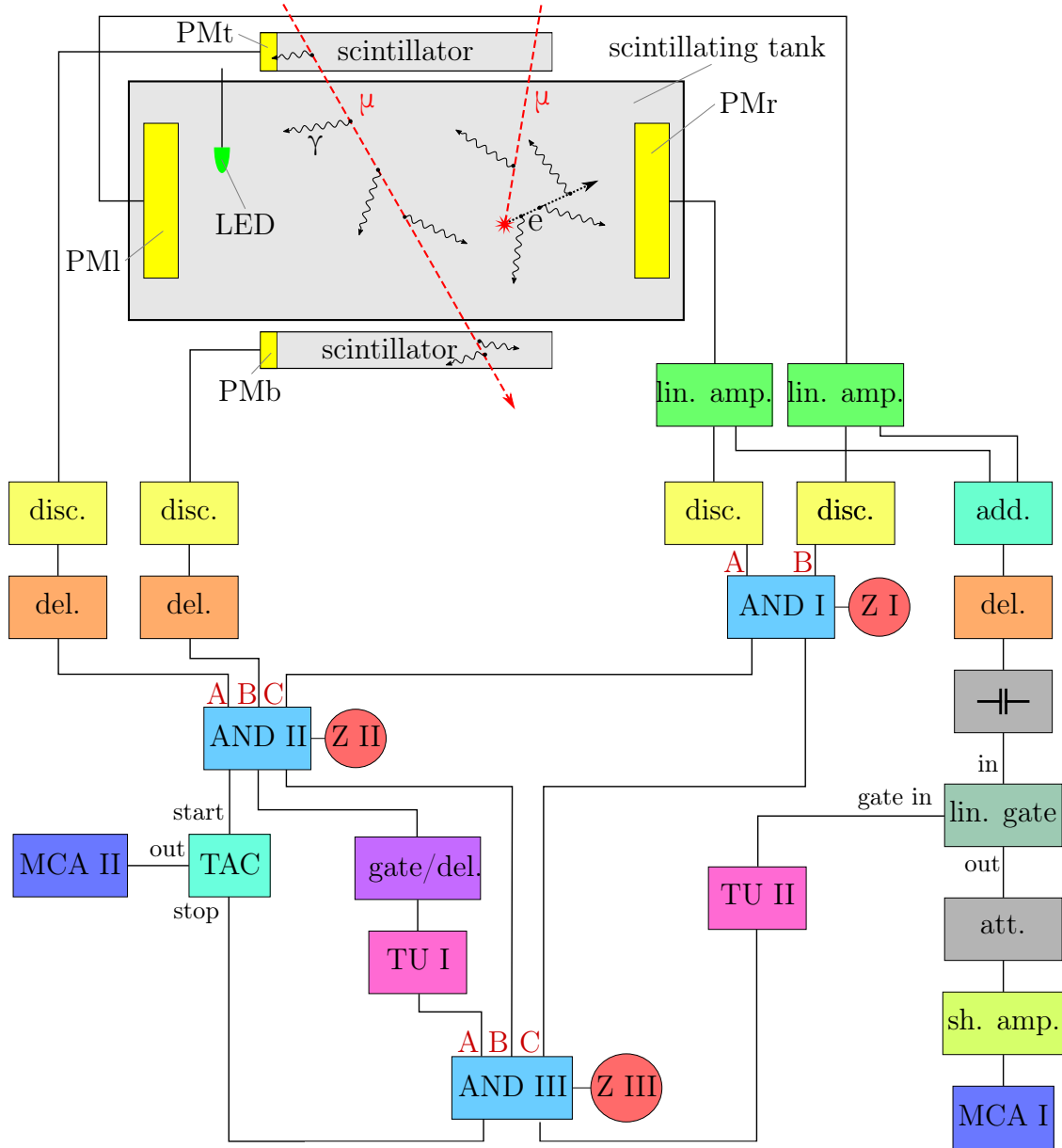


**Figure 3.1:** Experimental setup for the measurement of energy and decay time of cosmic muons. Muons are detected in a tank (filled with a scintillating fluid), causing flashes of light while flying through. The amount of light emitted is determined with photomultipliers, their signal then sent to a system of evaluating devices and recorded by multi channel analyzers.

**Figure 3.1** shows the setup that was used in the experiment. Its main part is a big metal tank filled with 470 l of a liquid scintillator. The flashes of light which are caused by the muons when they travel through the scintillator are measured with two photomultipliers located at the edges of the cylindrical tank (PMI and PMr). The signal from the two photomultipliers is then amplified with two *linear amplifiers*. The gain of the amplifiers is set to 2. From these amplifiers, the signal goes into *discriminators*. They only let pass signals with an amplitude exceeding an adjustable threshold. This threshold is set to a value which lets pass about 1000 pulses per second for each scintillator, in order to cut off underground noise but also to let through enough desired muon signals. The output signal of the discriminators is a rectangular pulse of about 50 ns length and -1.0 V amplitude. **Figure 3.2** shows a pulse from PMr (yellow), the amplified signal (blue) and the output of the discriminator (pink).

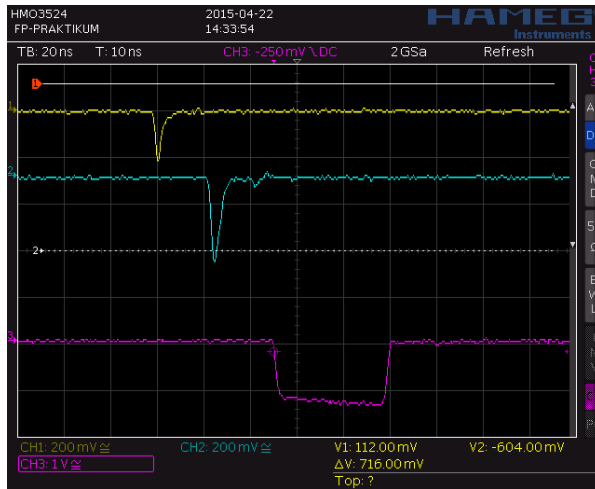


**Figure 3.2:** A muon passing through the scintillator causes a pulse of the photomultiplier PMr (yellow), the signal is then amplified (blue) and passes the discriminator which provides a rectangular output signal (pink).

The signals of the two discriminators are collected in a *coincidence unit* (AND I). The output signal of the coincidence unit is also a digital pulse like the one of the discriminators and it is triggered only if two signals from the discriminators reach its inputs simultaneously. This configuration again blocks a lot of undesired underground signals, since it is assumed that a muon passing the tank will generate a signal in both photomultipliers at once. A counter (Z I) after the coincidence unit permits the determination of the number of coinciding signals over a specific period. **Figure 3.3** shows a sample of those signals (the signal from the discriminators in yellow and blue and the output of the coincidence unit in pink).

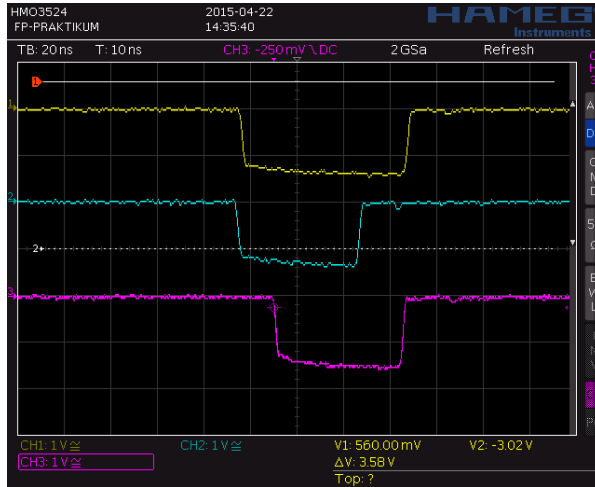


**Figure 3.3:** Coinciding signals from the discriminators (yellow and blue) create a pulse of the coincidence unit AND I (pink).

In order to determine the energy of the muon, the analog signals of the linear amplifiers also take a second way in the circuit: The signals are *added* and then delayed by 170 ns in a *delay generator* (to await analysis of the signals in a different part of the setup, this will become clear later). [Figure 3.4](#) shows the described signals, from the amplifiers in yellow and blue, the sum signal in pink and the delayed signal in green.

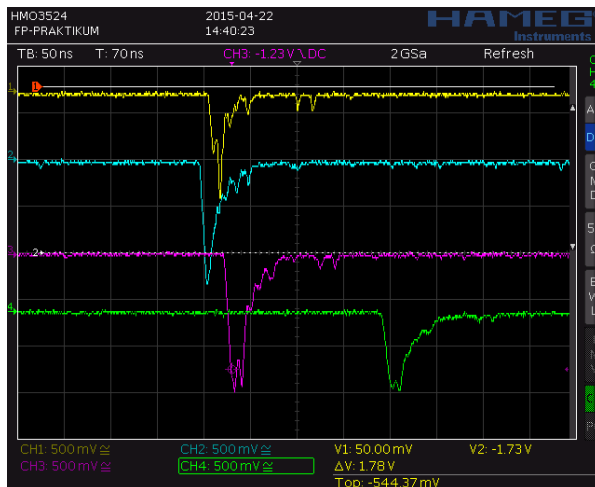


**Figure 3.4:** A muon causes peaks after the amplifiers (yellow and blue). The peaks are added (pink) and delayed (green).

After the delay generator, the signal goes over a *capacitor* (to block the constant component of the signal) and into a *linear gate*. The control signal for the gate comes from a different part of the setup and gets triggered if the approach of a muon has been detected

in the scintillating tank. Figure 3.5 shows a signal before the capacitor (yellow), after it (blue), the control signal for the linear gate (pink) and the output signal of the gate (green). On the figure it can be seen clearly that a signal can only pass the gate if it is open: The first peak of the blue signal can not pass, but the second runs through the gate, since it is opened by the pink pulse. The additional two small peaks of the green signal occur due to the opening and closing of the gate and constitute the main cause of the *pedestal* which is measured in the course of the experiment. *Pedestal* refers to the nonzero amplitude coming from the linear gate after opening even if there is no incoming signal.

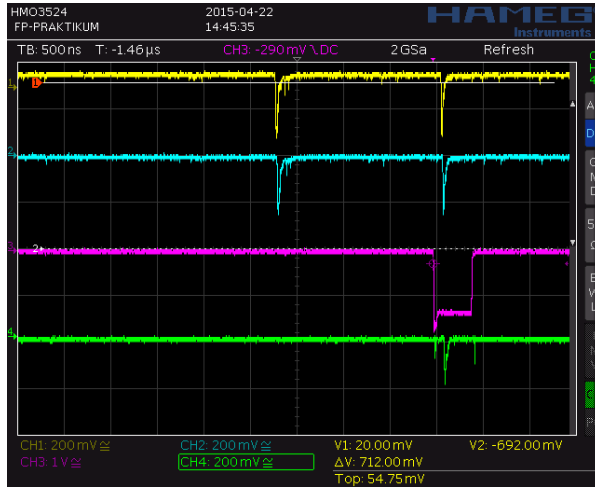
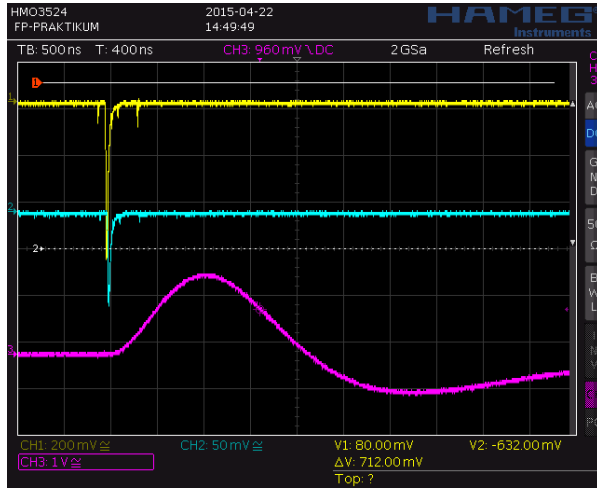


**Figure 3.5:** Signature of muon decay in the tank: The first peak is caused by the incoming muon, the second by the electron originating in the decay of the muon after  $1.8 \mu\text{s}$ . The signals are measured before the capacitor (yellow) and after the capacitor (blue). The control signal for the linear gate is depicted in pink and the output of the linear gate in green. The first signal can not pass the gate because the control signal is not supplied.

An *attenuator* after the linear gate damps the signal. The attenuation for the main measurement is 12 dB in order not to overload the following *shaping amplifier* which shows nonlinear behaviour above an input signal of about 100 mV.

Figure 3.6 shows the signal from the linear gate (yellow), the attenuated signal (blue) and the signal from the shaping amplifier (pink). The shaping amplifier integrates and differentiates its input signal and yields an output signal whose maximum amplitude is proportional to the charge of the input signal.

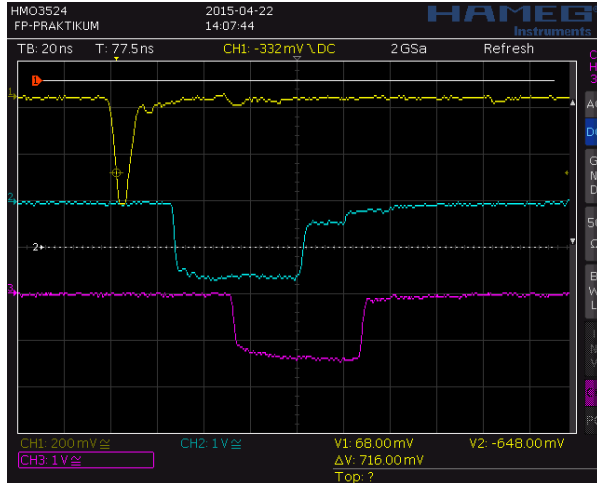
After the shaping amplifier a *multi channel analyzer* ranks the pulses by their amplitude and sends the data to a computer.



**Figure 3.6:** Signal from the linear gate (yellow), attenuated signal (blue) and signal after the shaping amplifier (pink). The amplitude of this signal contains information about the energy of the muon.

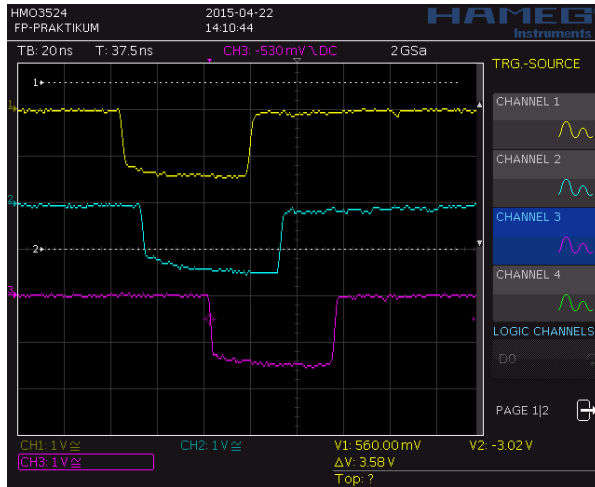
To generate the control signal for the linear gate, additional units are necessary: Two more scintillators with photomultipliers over and under the tank (PM<sub>t</sub> and PM<sub>b</sub>) detect the approach (and the flight through) of muons. Here again two discriminators are used to block small signals. The discriminator levels are set to values which lead to about 200 counts per second. After the discriminators, the signal is delayed by 25 ns to keep in time with the other components of the setup.

Figure 3.7 shows a pulse of the photomultiplier over the tank (yellow), the signal after the discriminator (blue) and the delayed signal (pink).



**Figure 3.7:** Signal from the photomultiplier over the tank (yellow), digital signal after the discriminator (blue) and delayed signal (pink).

The signal from the photomultiplier under the tank is processed the same way and the signals from the two delay generators go into another coincidence unit (AND II), together with the output of AND I. The inputs of AND II can be switched off and on, thus it can be defined which input conditions are necessary to trigger an output signal of AND II. The assignment of the inputs A, B and C can be seen on [Figure 3.1](#). The counter Z II counts the events after AND II. [Figure 3.8](#) shows input (yellow and blue) and output signal (pink) of AND II.



**Figure 3.8:** A muon flying through the tank causes two coinciding signals (yellow and blue) going into the coincidence unit AND II. The output signal is in pink.

The output signal of AND II is delayed by 500 ns in a *gate/delay generator*. This delay is necessary to avoid the incorrect identification of a passing muon as a decaying muon in a following section of the setup. The gate/delay generator triggers the opening of a  $7.5\ \mu\text{s}$  wide window in the subsequent *timing unit*. The signals are shown on [Figure 3.9](#): The pulse after AND II in yellow, the delayed pulse from the gate/delay generator in blue and the window of the timing unit in pink.

The signal of the timing unit (which occurs once the intrusion of a muon in the tank is detected) then goes into another coincidence unit AND III (input A). During the wide window of the timing unit the decay of the muon can cause a signal of the coincidence unit AND I. This signal also goes into AND III (yellow on [Figure 3.10](#)). After AND III (pink), another timing unit with a window of 400 ns provides the opening signal for the linear gate (green).

For the flight through measurement it is possible to shortcut the gate/delay generator and the timing unit and to pass the signal of AND II directly into AND III (input B). Events of AND III are counted with the counter Z III.

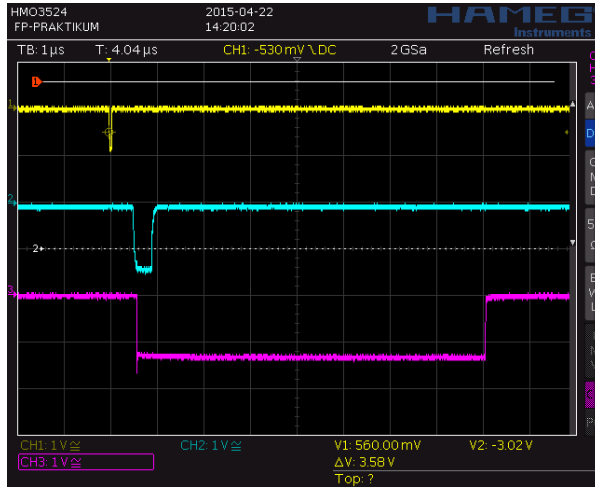


**Figure 3.9:** Pulse after the coincidence unit AND II (yellow), delayed signal after the gate/delay generator (blue) and 7.5  $\mu$ s-window of the timing unit (pink).

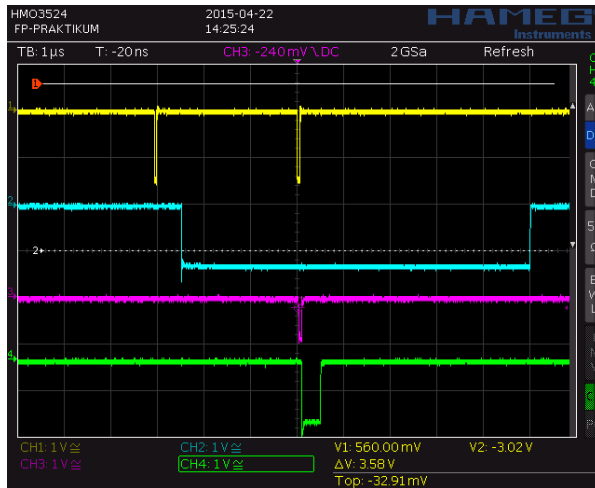


**Figure 3.10:** Creation of the control signal for the linear gate (green): The coincidence unit AND I records two events (yellow), the first event arising from the intrusion of a muon in the tank. This triggers a wide window of the timing unit I (blue) which allows the second pulse of AND I due to the decay of the muon to pass through AND III (pink). The signal of AND III opens a window after the timing unit II (green).

For the measurement of the decay time of muons a *time to amplitude converter* is used. It provides a signal whose amplitude is proportional to the time difference between a start and a stop signal. The start signal is delivered by the coincidence unit AND II when a muon enters the tank. The stop signal comes from AND III when a decay is recorded. The output of the TAC goes into a multi channel analyzer which is connected

to a computer. The signals for and from the TAC are shown on [Figure 3.11](#).

To perform the time calibration of the TAC, a special device is provided to generate start and stop pulses with adjustable time difference.

For the determination of the energy resolution of the setup a LED is integrated in the tank. The LED is controlled with a pulse generator and a LED driver.

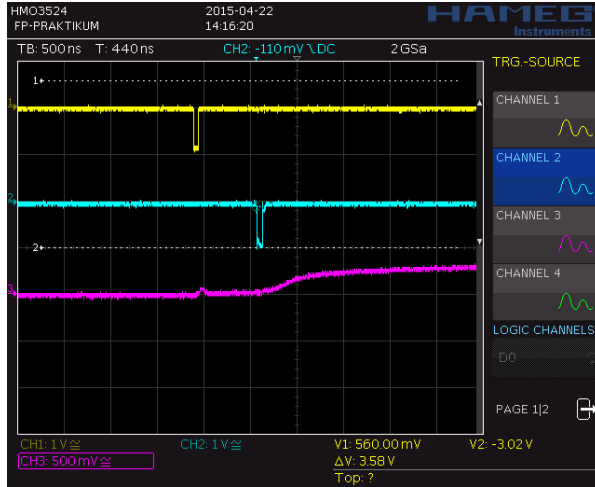


**Figure 3.11:** Signals at the time to amplitude converter: Start (yellow), stop (blue) and output (pink).

To verify the correct operation of the system after setting it up and during the days of the measurements, the count rates of the four photomultipliers and the coincident events were monitored regularly. [Table 3.1](#) shows the values that were determined after the successful completion of the setup.

**Table 3.1:** Count rates at various configurations of the setup.

	counter	AND I	AND II	AND III	counts	count rate <sup>6</sup> / s <sup>-1</sup>
PMr	Z I	A	-	-	141443/100 s	<b>1414 ± 4</b>
PMl	Z I	B	-	-	78865/100 s	<b>789 ± 3</b>
PMt	Z II	-	A	-	16640/100 s	<b>166.4 ± 1.3</b>
PMb	Z II	-	B	-	17181/100 s	<b>171.8 ± 1.3</b>
PMr & PMl	Z I	A B	-	-	106649/1000 s	<b>106.7 ± 0.3</b>
PMt & PMb	Z II	-	A B	-	108/100 s	<b>1.08 ± 0.10</b>
t & r & l	Z III	A B	A C	B C	20990/1000 s	<b>20.99 ± 0.14</b>
t & b & r & l	Z III	A B	A B C	B C	973/1000 s	<b>0.97 ± 0.03</b>
decays	Z III	A B	A C	A C	213/1000 s	<b>0.213 ± 0.014</b>
underground <sup>7</sup>	Z III	A B	A C	A C	16/1000 s	<b>0.016 ± 0.004</b>

## 4. Experimental procedure

### 4.1. Energy resolution: Photoelectronstatistics

For the determination of the energy resolution of the setup, the LED in the tank is used. [Table 4.1](#) shows the inputs of the coincidence units that are switched on during the measurements. A pulse generator produces a periodic signal with a frequency of 5 kHz. The signal is delivered to a LED driving unit, where the intensity of the LED can be adjusted. Twelve measurements with different intensities are conducted, in order to cover the whole energy range of the MCA I. The duration of each measurement is 1 min. For the three lowest intensities, the measuring time is increased to 6 min, 3 min and 2 min to reduce the error on the count rate. Each measurement produces an energy spectrum on MCA I which is saved.

**Table 4.1:** Active inputs of the coincidence units during measurement of the energy resolution of the setup.

coincidence unit	active inputs
AND I	A B
AND II	-
AND III	C

<sup>6</sup>The errors were calculated with Gaussian uncertainty propagation, assuming a Poisson distribution of the error on the number of counts (see section [5.1.1](#)).

<sup>7</sup>For the measurement of the underground, the gate/delay time was increased by a factor of 100.

## 4.2. Energy calibration

### 4.2.1. Pedestal measurement

[Table 4.2](#) shows the state of the setup for the measurement of the pedestal. Due to this wiring, the linear gate is opened each time a signal from PMt is delivered. As only about every 8th event from PMt coincides with an event of PMr and PMl ([Table 3.1](#)), in this configuration most likely no signal will pass the gate when it is opened. Such events give rise to the pedestal, a large peak at the low end of the spectrum measured with MCA I. After minimizing the pedestal with the offset screws on the delay generators, the pedestal is measured for 5 min.

**Table 4.2:** Active inputs of the coincidence units during measurement of the pedestal.

coincidence unit	active inputs
AND I	-
AND II	A
AND III	B

### 4.2.2. Recording of the flight through spectra

[Table 4.3](#) shows the settings of the coincidence units during the measurement of the flight through spectra for the energy calibration. In order to assign energy values to the channels of MCA I, three measurements with different attenuation are conducted. Attenuation and the duration of the measurements are given in [Table 4.4](#). The measurement at 35% signal strength is done to increase the accuracy of the energy calibration near the expected energy of the peak of the  $\beta$ -spectrum.

**Table 4.3:** Active inputs of the coincidence units during measurement of the flight through spectra.

coincidence unit	active inputs
AND I	A B
AND II	A B C
AND III	B C

**Table 4.4:** Attenuation and duration for the measurements of the flight through spectra.

measurement	signal strength	attenuation	duration
1	100%	12 dB	16 h
2	50%	18 dB	16.5 h
3	35%	21 dB	3.5 h

#### 4.2.3. Verification of the attenuator

In order to verify the proper functioning of the attenuator, a rectangular signal is fed to the attenuator, damped and the resulting amplitude measured with the oscilloscope. Measurements are conducted for 0 dB attenuation (as a reference) and for the attenuations of 12 dB, 18 dB and 21 dB.

### 4.3. Time calibration

The time calibration of the TAC and the MCA II is performed with a signal generator, which supplies two pulses with adjustable time difference on its two outputs. The outputs are connected to the input and the output of the TAC and the signal of the MCA is recorded. On the oscilloscope, the time difference between input and output signal is measured. Four measurements with time differences between 2  $\mu\text{s}$  and 8  $\mu\text{s}$  are done. The duration of one measurement is 10 min.

### 4.4. Underground measurement

[Table 4.5](#) shows the settings of the coincidence units for the measurement of the underground signal that occurs during the measurement of the  $\beta$ -spectrum and the determination of the muon lifetime. To ensure that only statistical events are recorded, the delay of the gate/delay generator is increased by a factor of 100 to 50  $\mu\text{s}$ . The underground is measured for 5.5 h.

The underground signal was only recorded for the energy measurement, since the underground for the determination of the decay time is negligible. This is due to the very low count rate of the underground ( $0.016 \pm 0.004 \text{ s}^{-1}$ , [Table 3.1](#)). As the TAC is active for just 10  $\mu\text{s}$  after it has been started, the probability  $p_u$  that during this time an underground signal in the TAC occurs is

$$p_u = 10 \mu\text{s} \cdot 0.016 \text{ s}^{-1} = 1.6 \cdot 10^{-7} . \quad (4.1)$$

The TAC is started about 21 times per second ([Table 3.1](#)), so for the underground count rate  $c_u$  we get

$$c_u = 21 \text{ s}^{-1} \cdot 1.6 \cdot 10^{-7} = 3.4 \cdot 10^{-6} \text{ s}^{-1} . \quad (4.2)$$

This is one count every 3 days.

**Table 4.5:** Active inputs of the coincidence units during measurement of the underground signal, the  $\beta$ -spectrum and the muon lifetime.

coincidence unit	active inputs
AND I	A B
AND II	A C
AND III	A C

## 4.5. The $\beta$ -spectrum and the mean lifetime

For the main measurement, the configuration of the coincidence units is shown in [Table 4.5](#). The  $\beta$ -spectrum is collected in the MCA I, the decay time of the muon in MCA II. The measurement runs for 65 h.

## 4.6. Schedule of the experiment

The above description of the various parts of the experiment is arranged in a logical order. The actual execution followed a different order which is given in [Table 4.6](#).

**Table 4.6:** Schedule of the experiment.

day	activity
Monday	connection of devices, examination of signals with oscilloscope
Tuesday	testing of setup, solving a problem with a defective contact of the linear amplifier, taking pictures with oscilloscope
Wednesday	final testing, measuring of count rates, time calibration (1 h), attenuator calibration, flight through spectrum 100% (over night)
Thursday	pedestal (5 min), underground (5.5 h), energy resolution (1 h), flight through spectrum 50% (over night)
Friday	test experiment $\beta$ -spectrum and mean lifetime (1 h), flight through spectrum 35% (3.5 h), $\beta$ -spectrum and mean lifetime (65 h)

## 5. Measurement results and evaluation

### 5.1. General remarks

#### 5.1.1. Errors and count rate

The number  $N$  of measurement events of a channel of the MCAs is Poisson distributed. Hence the error  $s_N$  of  $N$  events is:

$$s_N = \sqrt{N} \quad (5.1)$$

Not all measurements were done in the same amount of time, so we decided to normalize all measured data with the elapsed time  $t$  to a count rate  $n$ . Consequently the error changes, too:

$$n = \frac{N}{t}, \quad s_n = \frac{s_N}{t} \quad (5.2)$$

#### 5.1.2. Gaussian distribution

For some fits we use the Gaussian distribution. The following convention will be used:

$$\text{gaus}(c; x, \sigma) = e^{-\frac{1}{2}\left(\frac{c-x}{\sigma}\right)^2} \quad (5.3)$$

in which  $\text{gaus}(c; x, \sigma)$  is a function of  $c$  with parameters  $x$  (expectation value) and  $\sigma$  (standard deviation).

#### 5.1.3. Rebinning

Sometimes there is too much noise in the spectrum to recognize a trend. In those cases  $n$  successive  $(x, y)$  tuples are averaged:

$$\bar{x}_i = \frac{1}{n} \sum_{j=0}^{n-1} x_{ni+j}, \quad \bar{y}_i = \frac{1}{n} \sum_{j=0}^{n-1} y_{ni+j}, \quad i = 1, 2, \dots, \frac{\#(x_i)}{n} \quad (5.4)$$

where  $(x_i, y_i)$  are the old values and  $(\bar{x}_i, \bar{y}_i)$  are the new ones.  $\#(x_i)$  is the number of old values. The errors are calculated with error propagation:

$$s_{\bar{x}_i} = \frac{1}{n} \sqrt{\sum_{j=0}^{n-1} s_{x_{ni+j}}^2}, \quad s_{\bar{y}_i} = \frac{1}{n} \sqrt{\sum_{j=0}^{n-1} s_{y_{ni+j}}^2} \quad (5.5)$$

## 5.2. Energy resolution

The spectra for the energy resolution measurement are fitted with a Gaussian distribution and a constant offset:

$$n(c) = b + A \text{gaus}(c; x, \sigma) \quad (5.6)$$

An example fit is shown in [Figure 5.1](#). Ideally a line is expected, but because of the energy resolution it is blurred into a Gaussian distribution. The standard deviation  $\sigma$  of the Gaussian distribution is a measure for the energy resolution. From [Figure 5.2](#) can be seen that with increasing channel number the energy resolution decreases. All fitted standard deviations are plotted against the expectation value of their respective Gaussian distributions ([Figure 5.3](#)).

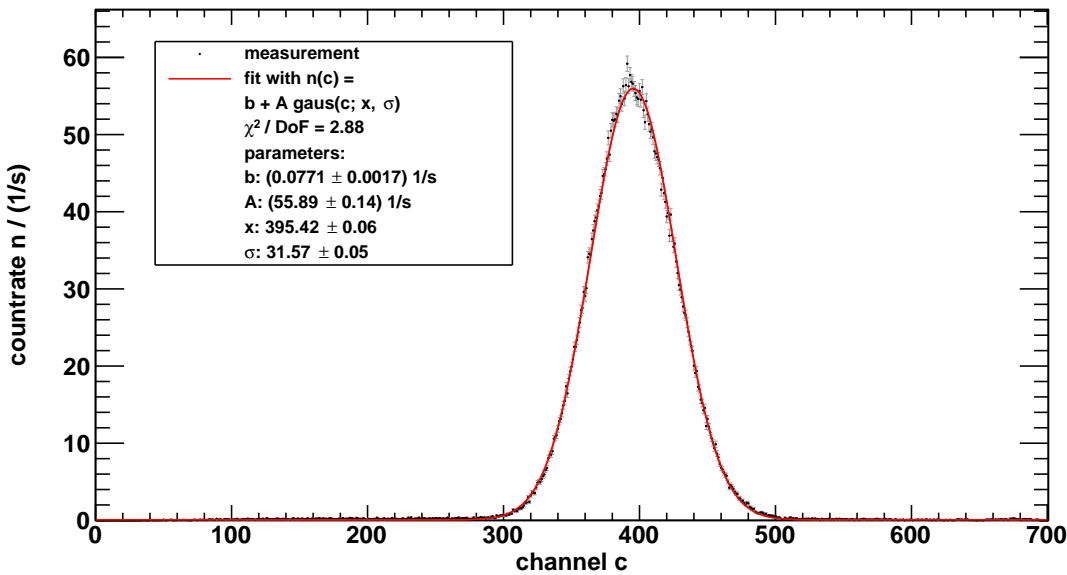


**Figure 5.1:** Recorded and fitted spectrum of the LED flashing in the tank for one minute with medium intensity.

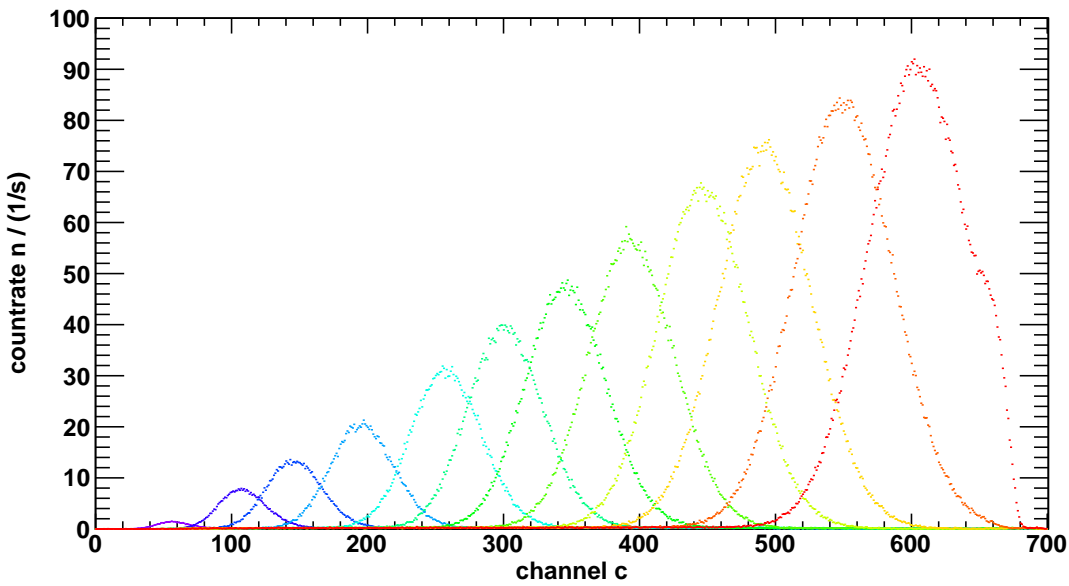


**Figure 5.2:** All measured energy spectra of the flashing LED in the tank. Raising the intensity of the LED increases the expectation value, the standard deviation (energy uncertainty) and the amplitude of the distributions.

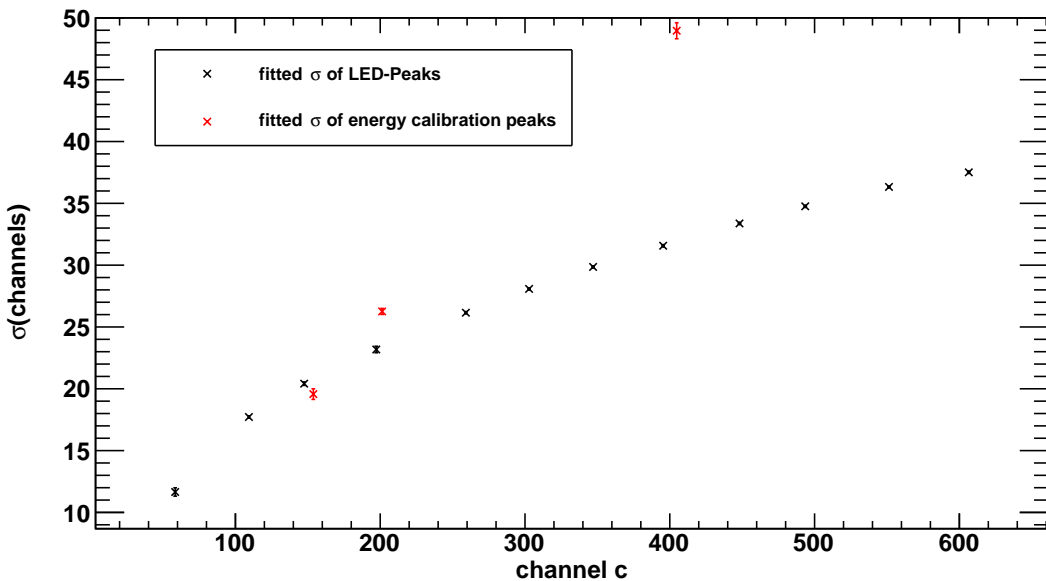


**Figure 5.3:** Fitted standard deviations plotted against the expectation value of their respective Gaussian distributions as seen in [Figure 5.2](#). The red points are the blurs of the flight through spectra (evaluated in section [5.3.2](#)).

### 5.3. Energy calibration

For the energy calibration the pedestal measurement and flight through spectra are evaluated. Then the theoretical energies are calculated and those two datasets are plotted against each other.

#### 5.3.1. Pedestal

The pedestal measurement produced a Gaussian distributed spectrum (Figure 5.4).

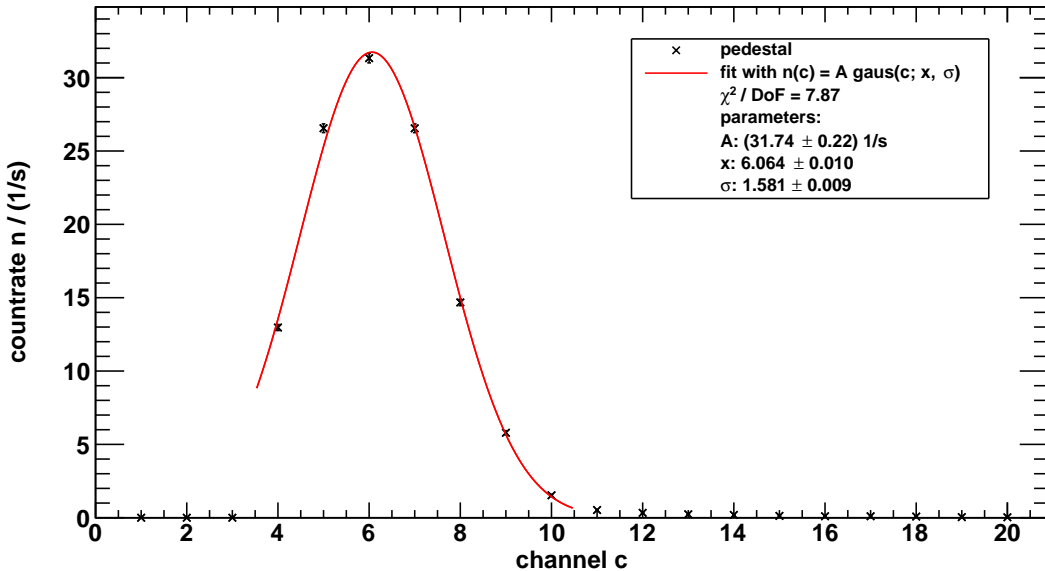


**Figure 5.4:** Pedestal: Peak at the low end of the energy spectrum caused by opening the linear gate without the occurrence of a passing signal. The reason for the pedestal is shown in Figure 3.5.

The peak is fitted with the Gaussian distribution multiplied by an amplitude  $A$ :

$$n(c) = A \cdot \text{gaus}(c; x, \sigma) \quad (5.7)$$

The expectation value of the fitted Gaussian distribution is:

$$x = (6.064 \pm 0.010) \quad (5.8)$$

#### 5.3.2. Flight through spectra

**Landau distribution** The Landau distribution describes the fluctuations of energy loss caused by impact ionization<sup>8</sup>. It has two parameters: The location parameter  $\mu$  which

<sup>8</sup>The distribution follows from the *Bethe formula*.

shifts the distribution in x-direction and the scale parameter  $s$  which controls the width of the distribution. The maximum of the distribution (most probable value,  $m$ ) is not equivalent with the location parameter but it can be calculated:

$$m = \mu + (-0.22278298) \cdot s \quad (5.9)$$

The value  $-0.22278298$  is the location of the most probable value if  $\mu = 0$ .

The measured data cannot be described by just a Landau distribution, since the spectrum is blurred by the energy resolution of the scintillator. To get a function for fitting a convolution of the Landau distribution with a Gaussian distribution is needed:

$$(\text{landau}(\mu, s) * \text{gaus}(0, \sigma))(c) = \int_{-\infty}^{\infty} \text{landau}(x; \mu, s) \text{gaus}(c - x; 0, \sigma) dx \quad (5.10)$$

Since there is no analytical closed form for the Landau distribution the convolution can not be solved analytical. The spectra are fitted with a numerical convolution<sup>9</sup>. The spectra with their fits are shown in [Figure 5.5](#), [Figure 5.6](#) and [Figure 5.7](#). Parameter  $A$  of the fit is the area under the curve and was needed for fitting, but is not relevant for the further evaluation. The fitted parameters are listed in [Table 5.2](#).

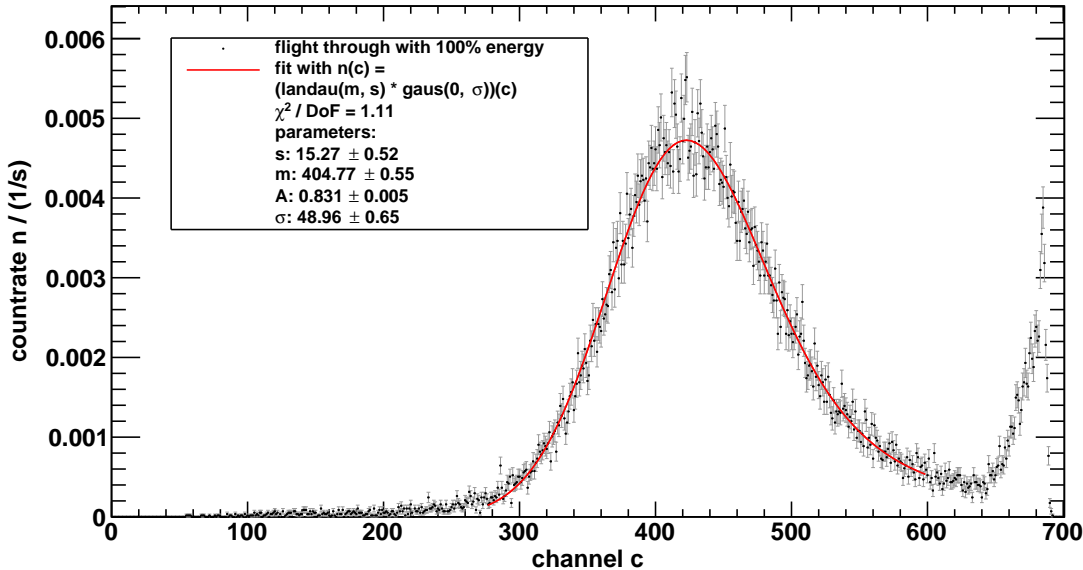


**Figure 5.5:** Flight through spectrum of muons with 12 dB attenuation ( $\triangleq 100\%$  energy) with a blurred Landau fit.

<sup>9</sup>The code is based on <https://root.cern.ch/root/html/tutorials/fit/langaus.C.html>, translated to Python by us.

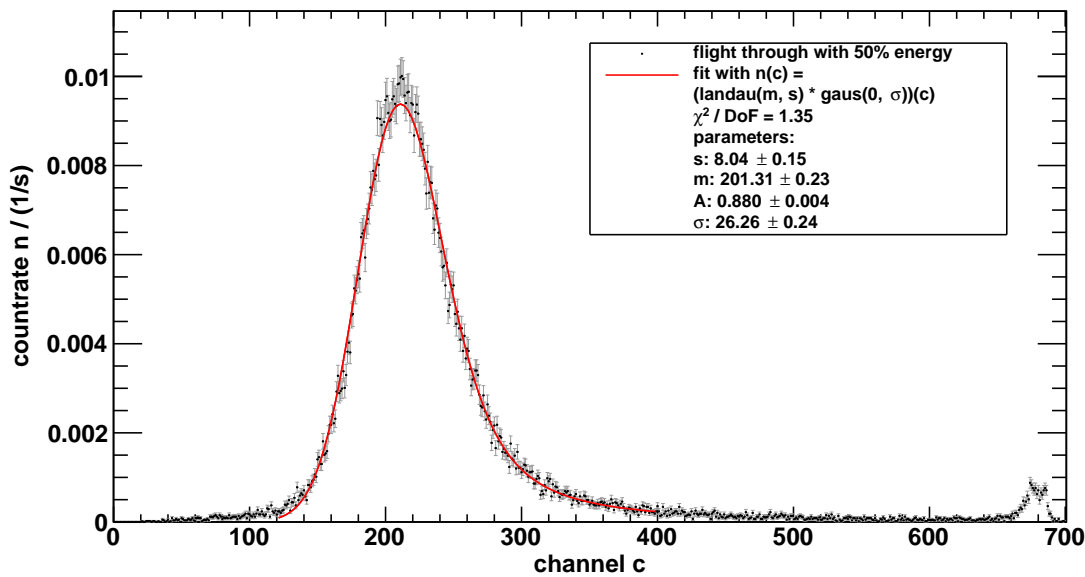


**Figure 5.6:** Flight through spectrum of muons with 18 dB attenuation ( $\triangleq 50\%$  energy) with a blurred Landau fit.

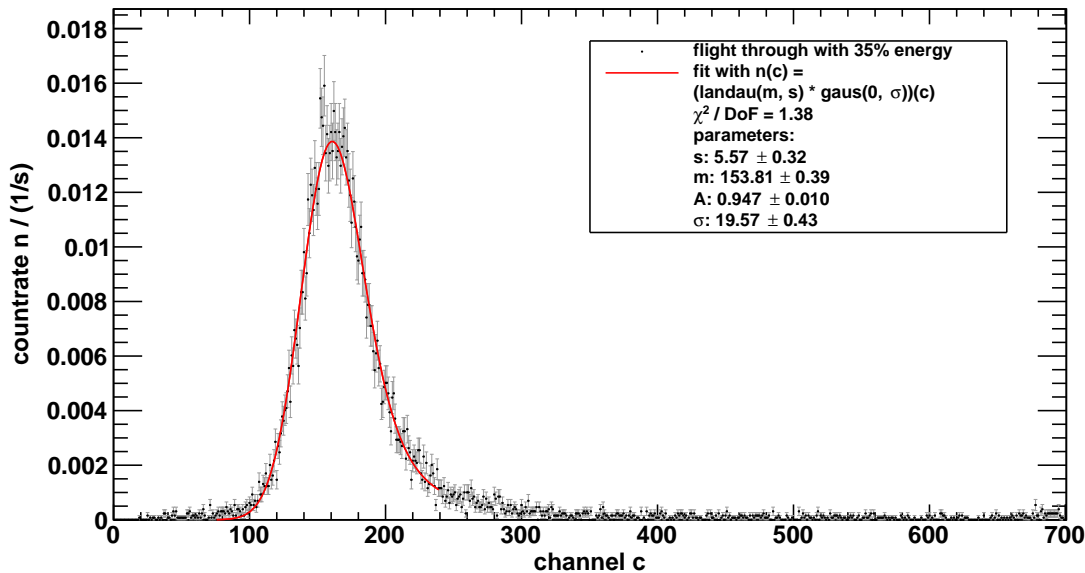


**Figure 5.7:** Flight through spectrum of muons with 21 dB attenuation ( $\triangleq 35\%$  energy) with a blurred Landau fit.

### 5.3.3. Verification of the attenuator

The measured amplitudes  $A$  of the attenuated signals are shown in [Table 5.1](#).

**Table 5.1:** Measured amplitude  $A$  of a periodic rectangular signal after the attenuation with nominal value  $n$ .

$n$ / dB	$A$ / mV	$s_A$ / mV
0	840	40
12	210	10
18	106	4
21	75	4

The measured attenuation  $m$  can be calculated with

$$m = -20 \log_{10} \left( \frac{A}{A_0} \right), \quad s_m = \frac{20}{\ln 10} \sqrt{\left( \frac{s_A}{A} \right)^2 + \left( \frac{s_{A_0}}{A_0} \right)^2} \quad (5.11)$$

where  $A_0$  is the the amplitude at  $n = 0$  dB. Those attenuations can be plotted against the nominal values ([Figure 5.8](#)).

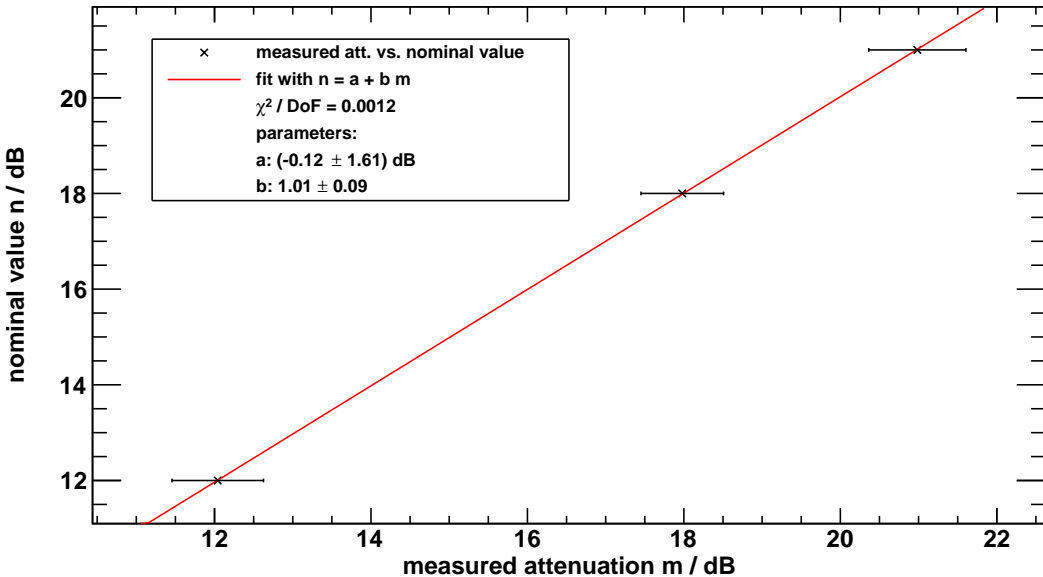


**Figure 5.8:** Nominal attenuations  $n$  plotted against the measured attenuations  $m$  and fit with a line.

If the attenuator works correctly, the linear fit should yield a line with intercept  $a = 0 \text{ dB}$  and slope  $b = 1$ . The fit results are:

$$\begin{aligned} a &= (-0.1 \pm 1.6) \text{ dB} \\ b &= 1.01 \pm 0.09 \end{aligned} \tag{5.12}$$

Therefore we conclude that the attenuator works correctly and no correction is needed.

### 5.3.4. Calibration

For the calibration it must be known how much energy a muon deposits in the tank. Following data was given:

$$\begin{aligned} \frac{\partial E}{\partial \rho x} &= (1.95 \pm 0.05) \frac{\text{MeV} \cdot \text{cm}^2}{\text{g}} && \text{(minimal ionizing muon)} \\ \rho &= (0.87 \pm 0.01) \frac{\text{g}}{\text{cm}^3} && \text{(density of solvent)} \\ s &= (84 \pm 5) \text{ cm} && \text{(mean free path in tank)} \end{aligned} \tag{5.13}$$

Hence the total loss of energy calculates to:

$$\begin{aligned} E &= \frac{\partial E}{\partial \rho x} \cdot \rho \cdot s = 142.5 \text{ MeV} \\ s_E &= E \cdot \sqrt{\left( \frac{s_{\frac{\partial E}{\partial \rho x}}}{\frac{\partial E}{\partial \rho x}} \right)^2 + \left( \frac{s_\rho}{\rho} \right)^2 + \left( \frac{s_s}{s} \right)^2} = 9.4 \end{aligned} \tag{5.14}$$

The percentage loss of energy can now be determined:

$$E_p = p \cdot E, \quad s_{E_p} = p \cdot s_E, \quad 0 \leq p \leq 1 \tag{5.15}$$

The fitted peaks of the energy calibration and their respective energies are listed in Table 5.2 and visualized in [Figure 5.9](#).

**Table 5.2:** Channels of fitted peaks and their theoretical energy for the energy calibration.

% energy	$c$	$s_c$	$E / \text{MeV}$	$s_E / \text{MeV}$
0	6.064	0.010	0.0	0.0
35	153.808	0.392	49.9	3.3
50	201.312	0.225	71.3	4.7
100	404.770	0.547	142.5	9.4

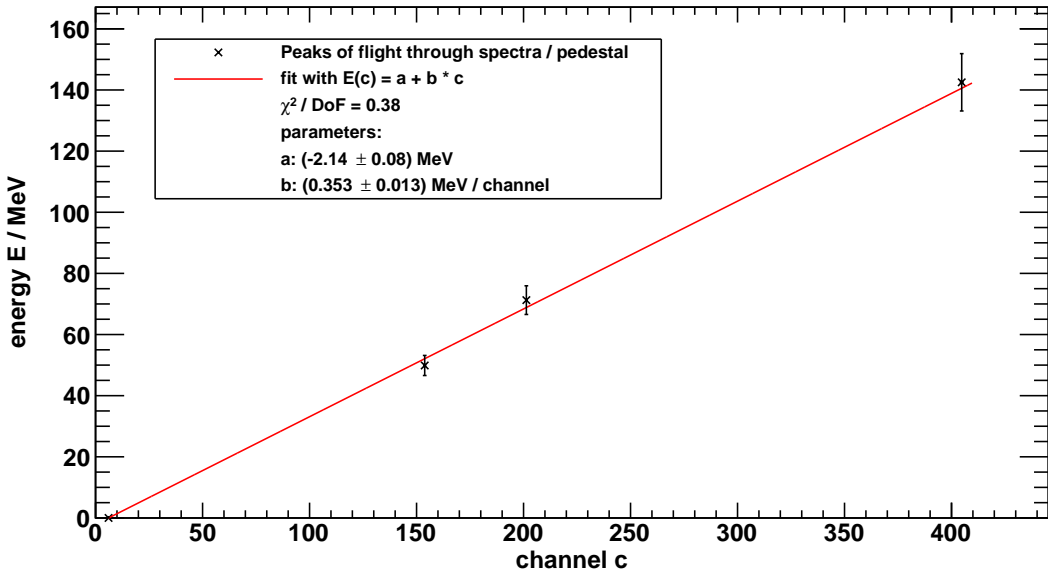


**Figure 5.9:** Amount of energy deposited in the tank during the 35%, 50% and 100% flight through measurement and the pedestal as a function of the spectrum's maximum position.

Since the scintillators should produce a signal amplitude linear to the measured energy, a linear fit is implemented:

$$E(c) = a + b \cdot c \quad (5.16)$$

The fit yields:

$$\begin{aligned} a &= (-2.14 \pm 0.08) \text{ MeV} \\ b &= (0.353 \pm 0.013) \frac{\text{MeV}}{\text{channel}} \\ \text{cov}(a, b) &= -0.0011 \frac{\text{MeV}^2}{\text{channel}} \end{aligned} \quad (5.17)$$

Now the energy  $E$  of a channel  $c$  and its error  $s_E$  can be calculated with:

$$E = a + b \cdot c, \quad s_E = \sqrt{s_a^2 + (c \cdot s_b)^2 + 2 \cdot c \cdot \text{cov}(a, b)} \quad (5.18)$$

## 5.4. Time calibration

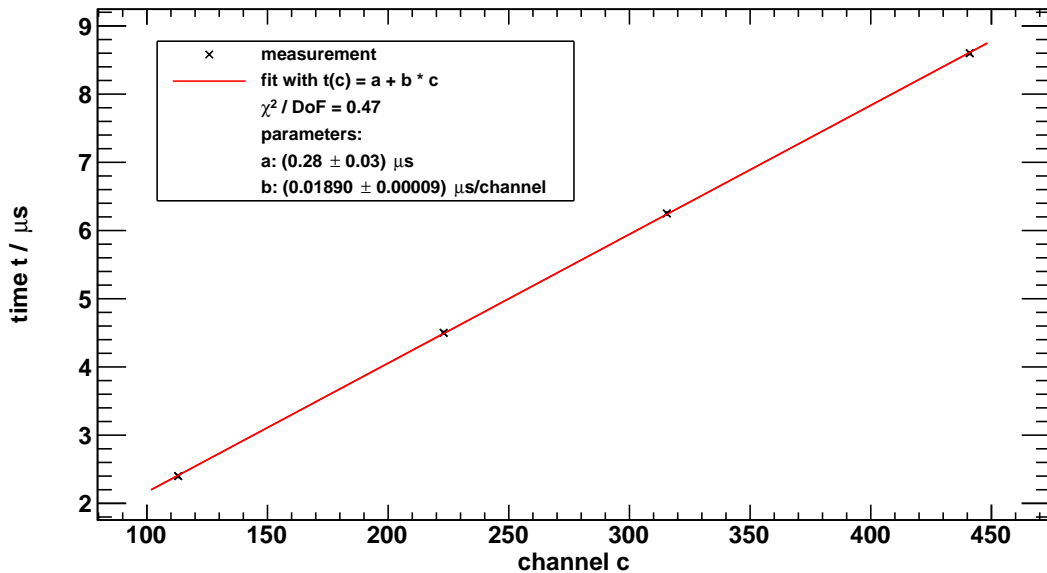
In Table 5.3 the data for the time calibration is listed. In each of the four measurements, there were only one or two channels of MCA II responding, so there is no need to fit the data.

**Table 5.3:** Measured times and channels with errors for the time calibration.

$t / \mu\text{s}$	$s_t / \mu\text{s}$	$c$	$s_c$
2.40	0.02	113.0	0.5
4.50	0.02	223.0	0.5
6.25	0.02	315.5	0.5
8.60	0.02	441.0	0.5

A linear fit is done (Figure 5.10):

$$t = a + b \cdot c \quad (5.19)$$

**Figure 5.10:** Time difference between the start and stop signal for the TAC as a function of the responding channel of MCA II.

The parameters and their covariance for this fit are:

$$\begin{aligned} a &= (0.28 \pm 0.03) \mu\text{s} \\ b &= (0.01890 \pm 0.00009) \frac{\mu\text{s}}{\text{channel}} \\ \text{cov}(a, b) &= -2.299 \frac{\mu\text{s}^2}{\text{channel}} \end{aligned} \quad (5.20)$$

Now the time  $t$  of a channel  $c$  and its error  $s_t$  can be calculated with:

$$t = a + b \cdot c, \quad s_t = \sqrt{s_a^2 + (t \cdot s_b)^2 + 2 \cdot t \cdot \text{cov}(a, b)} \quad (5.21)$$

## 5.5. Underground

The underground measurement is visualized in [Figure 5.11](#). Because many channels contain no event a rebinning is done with a bin size of 20 channels ([Figure 5.12](#)).

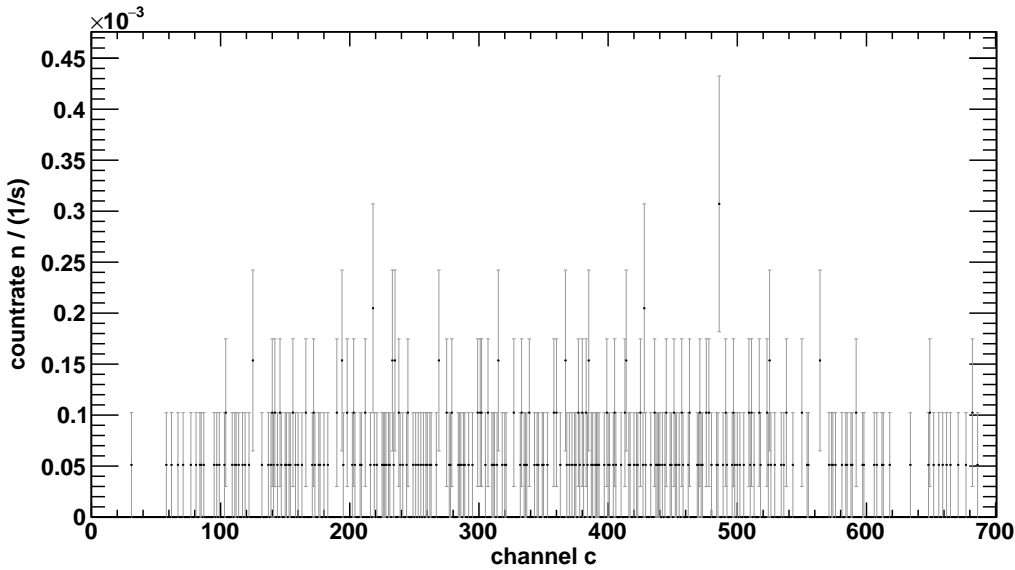


**Figure 5.11:** Underground signal during the measurement of the  $\beta$ -spectrum.

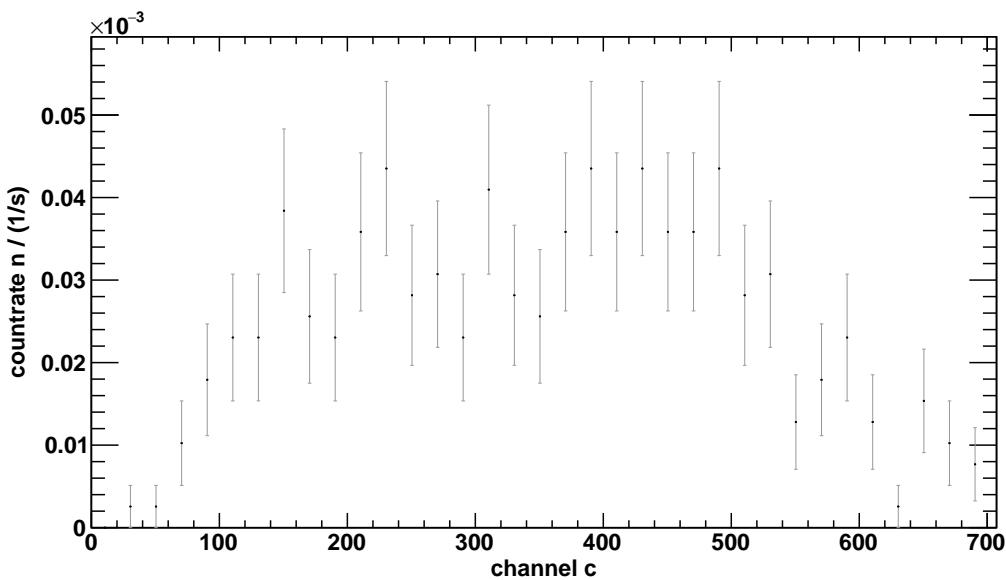


**Figure 5.12:** Underground signal during the measurement of the  $\beta$ -spectrum after a rebinning with bin size 20 channels.

## 5.6. $\beta$ -spectrum

The measured  $\beta$ -spectrum is shown in [Figure 5.13](#). By comparing the count rate of the underground ( $1.8 \cdot 10^{-5} \text{ s}^{-1}$ ) with the  $\beta$ -spectrum ( $2.1 \cdot 10^{-3} \text{ s}^{-1}$ ) at channel 90 (maximum of  $\beta$ -spectrum) one can see that the signal to noise ratio is about 116. The minimal relative error for the  $\beta$ -spectrum is  $\frac{1}{\sqrt{545}} \approx 4.3\%$  (545 counts were measured at the maximum). Therefore the underground is not the main source of uncertainty and can be neglected.

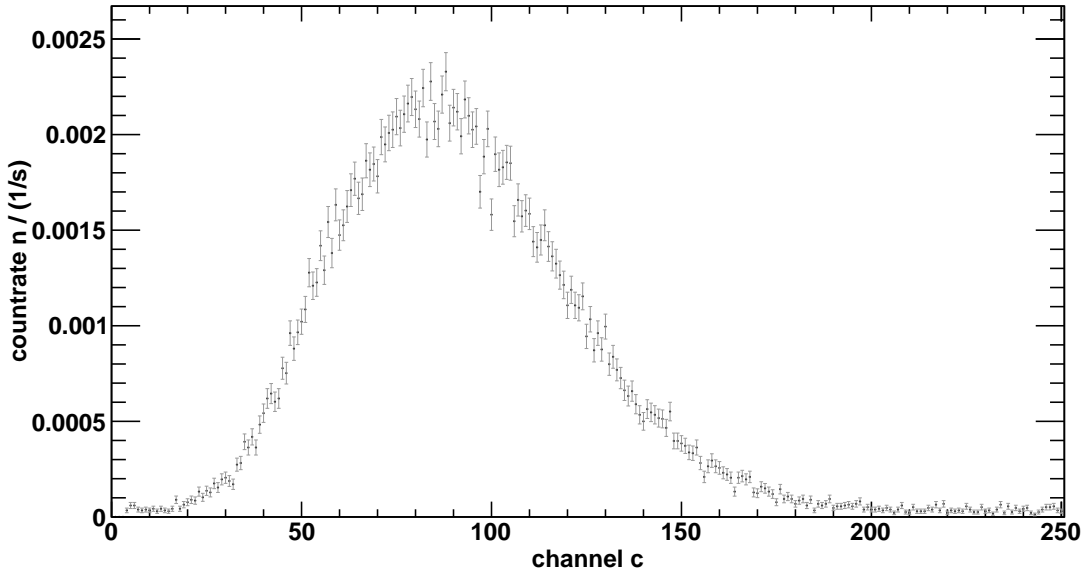


**Figure 5.13:** Main measurement of the experiment: The  $\beta$ -spectrum of the muon decay.

The problem is to extract the maximal energy of the  $\beta$ -spectrum while taking the Gaussian blur caused by the energy resolution into account. One method is the *Fermi-Kurie-plot* ([2], p.52-53). First the channel information is converted into an energy with [Equation 5.18](#). Then  $\sqrt{n(E)/E^2}$  is plotted against the energy  $E$  ([Figure 5.14](#)). Ideally a linear relationships should be identifiable. The intersection of this line with the  $x$ -axis is the maximal energy. Because of the Gaussian blur only a part of the plot is linear. This part gets fitted with

$$\sqrt{n(E)/E^2} = a(E - b), \quad (5.22)$$

so that the intersection with the  $x$ -axis can be read directly.

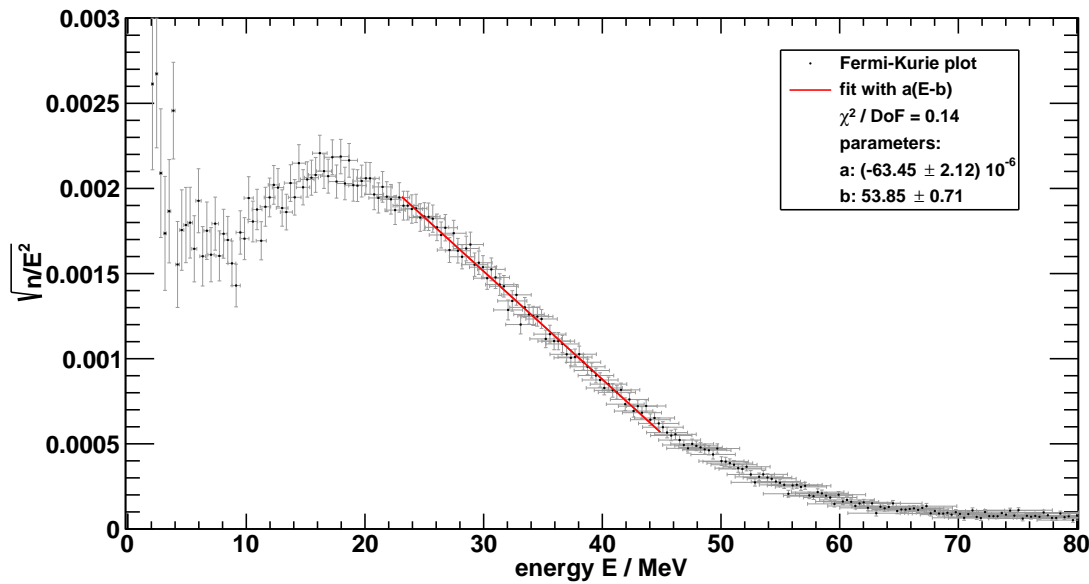


**Figure 5.14:** Fermi-Kurie plot of the  $\beta$ -spectrum.

With the fit one gets for  $b$ :

$$b = (53.85 \pm 0.71) \text{ MeV} \quad (5.23)$$

Since this energy is half of the rest energy of the muon (neglecting the mass of the electron) it has to be multiplied with 2:

$$\begin{aligned} E_\mu &= 2 \cdot b, & s_{E_\mu} &= 2 \cdot s_b \\ \Rightarrow E_\mu &= (107.7 \pm 1.4) \text{ MeV} \end{aligned} \quad (5.24)$$

The so calculated rest energy matches the literature value ([Equation 2.1](#)) within a  $2\sigma$ -interval.

$$E_\mu^{\text{lit.}} = (105.6583715 \pm 0.0000035) \text{ MeV} \quad (5.25)$$

## 5.7. Mean lifetime

To calculate the mean lifetime  $\tau_\mu$  of the muon the channels are converted to a time with [Equation 5.21](#). Furthermore we rebin with a bin size of three the spectrum as described in [5.1.3](#) to get a nicer curve.

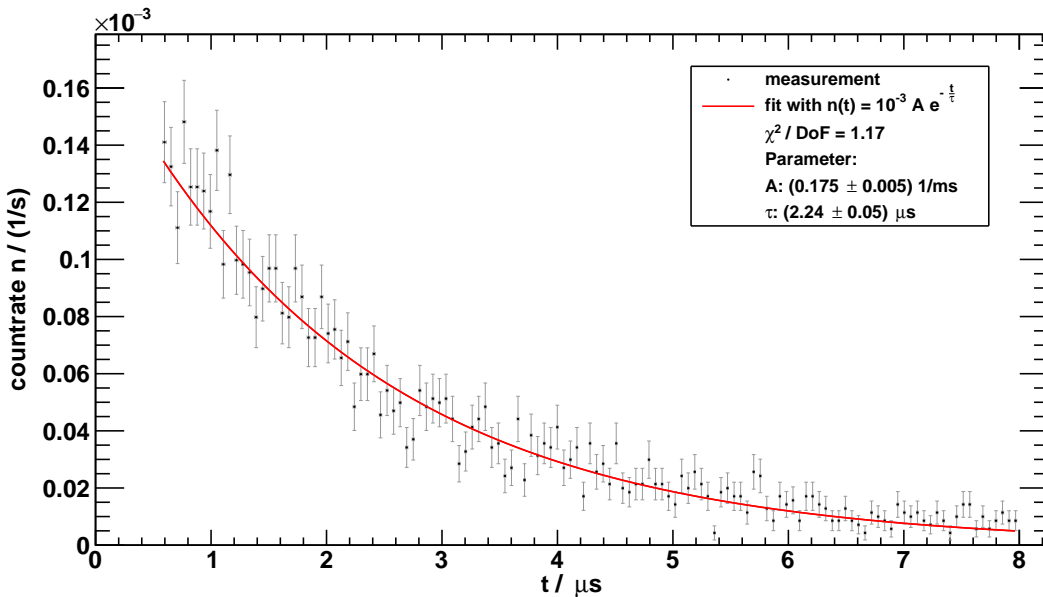


**Figure 5.15:** Count rate  $n$  of muon decays as a function of lifetime  $t$ .

The so obtained datapoints ([Figure 5.15](#)) get fitted with an exponential function, since they obey the law of decay ([2.2.1](#)):

$$n = A \cdot e^{-\frac{t}{\tau}} \quad (5.26)$$

The fit yields for the mean lifetime:

$$\tau_\mu = (2.24 \pm 0.05) \mu\text{s} \quad (5.27)$$

This matches with the literature value ([Equation 2.2](#)) within  $1-\sigma$ -interval.

$$\tau_\mu^{\text{lit.}} = (2.1969811 \pm 0.0000022) \mu\text{s} \quad (5.28)$$

## 5.8. Weak coupling constant

Now the weak coupling constant  $G_\mu$  can be calculated with the muon's mass and mean lifetime. [Equation 2.11](#) is used. The calculation is performed in natural units:

$$\begin{aligned} G_\mu &= \sqrt{\frac{192\pi^2}{\tau_\mu m_\mu^5}} \\ s_{G_\mu} &= \frac{1}{2} \sqrt{\frac{192\pi^3 (m_\mu^2 s_{\tau_\mu}^2 + 25\tau_\mu^2 s_{m_\mu}^2)}{m_\mu^7 \tau_\mu^3}} \end{aligned} \quad (5.29)$$

With the relation

$$t_{\text{natural}} = \frac{1}{\hbar} t_{\text{S.I.}} \quad (5.30)$$

the mean lifetime can be converted to natural units.  $\hbar$  has to be in eVs.

The weak coupling constant calculates to:

$$G = (1.10 \pm 0.04) \cdot 10^{-5} \frac{1}{\text{GeV}^2} \quad (5.31)$$

This result agrees with the literature value ([Equation 2.12](#)) within  $2\sigma$ -interval.

$$G_\mu^{\text{lit.}} = (1.166364 \pm 0.000005) \cdot 10^{-5} \frac{1}{\text{GeV}^2} \quad (5.32)$$

## References

- [1] DESY-Praktikum der Universität Hamburg: *Kosmische Strahlung, Summary, Literaturmappe zum Praktikumsversuch "Lebensdauer von Myonen"*.
- [2] Demtröder, W. *Experimentalphysik 4, Kern-, Teilchen- und Astrophysik, 3. Auflage*. Springer Spektrum, 2010.
- [3] Träris, A. *Simulation und Vorversuche zur Messung des Betaspektrums nach dem Myonzerfall; Staatsexamsarbeit*. Freiburg, 1993.

## A. Appendix

### A.1. Lab report

# Myos - Protokoll

Mo Aufbau Schaltung

Problem linear Gute

Di Aufbau Schaltung

Test Schüle

Delay zw. Bmteren

=>

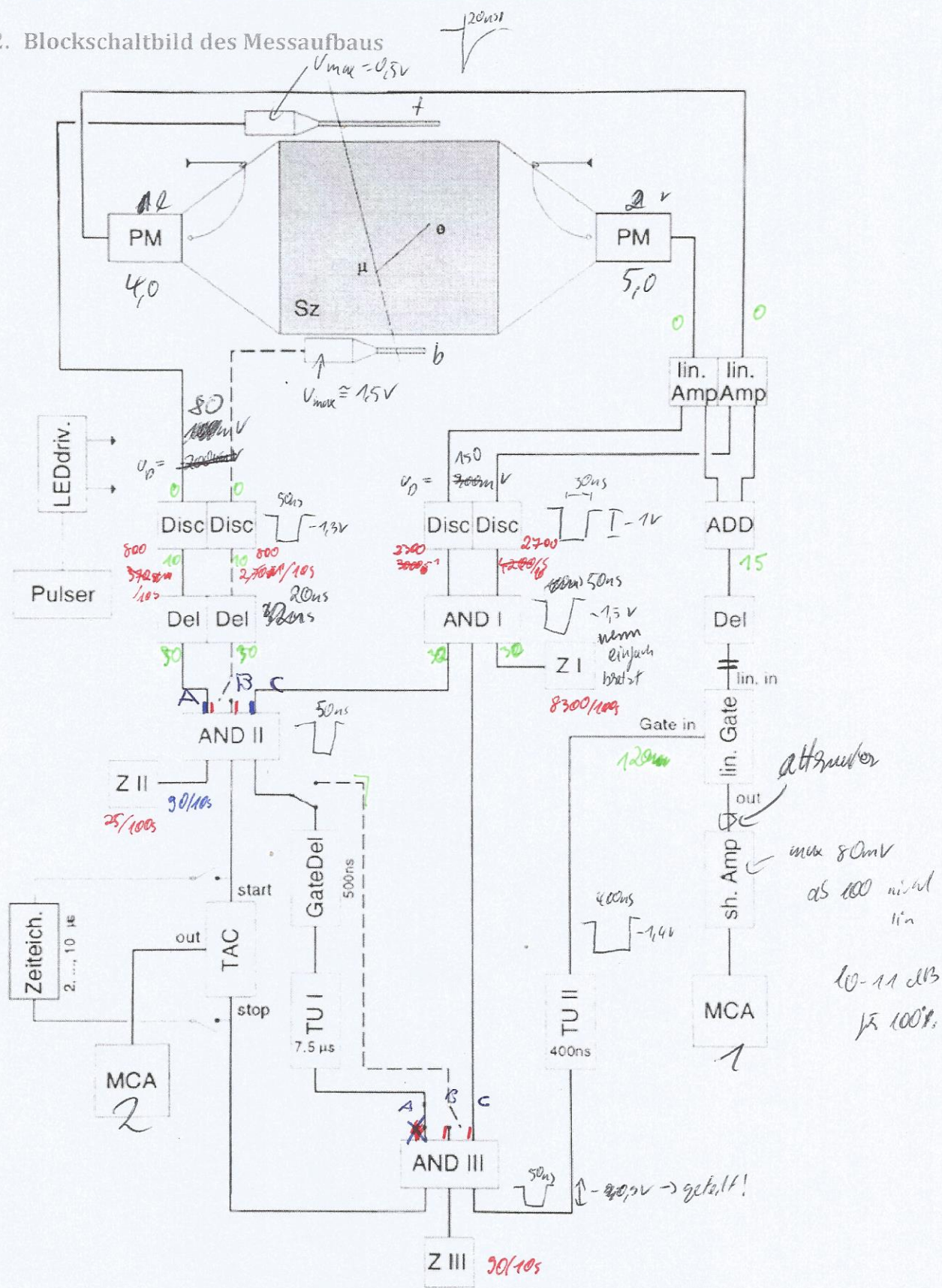
nekte Ausl

Tutor's Sign

Mo

24/03/15

## 2. Blockschaltbild des Messaufbaus



# Mi Zeitreihung:

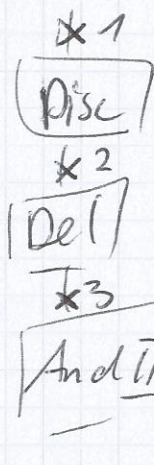
Zeit	mit 1μs	Fch	Bild
2μs	$2,4 \pm 0,1$	113	50001
4μs	$4,5 \pm 0,1$	223	50002
6μs	$6,25 \pm 0,1$	375,5	50003
8μs	$8,6 \pm 0,1$	441	50004
10μs	$10,6 \pm 0,1$	-	50005

# Photos

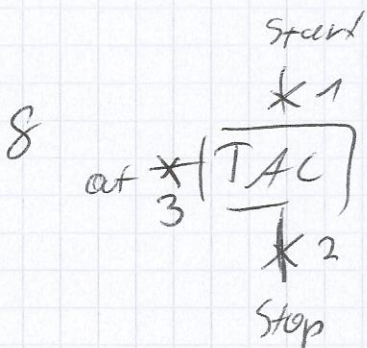
n

6

was Fop



7

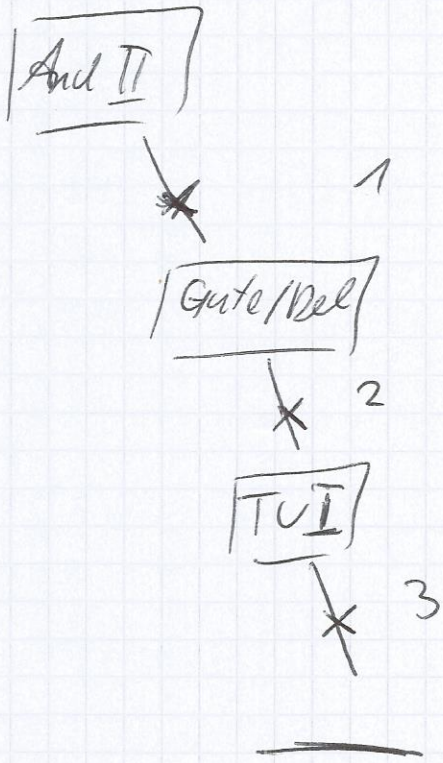


Tutor's wgn

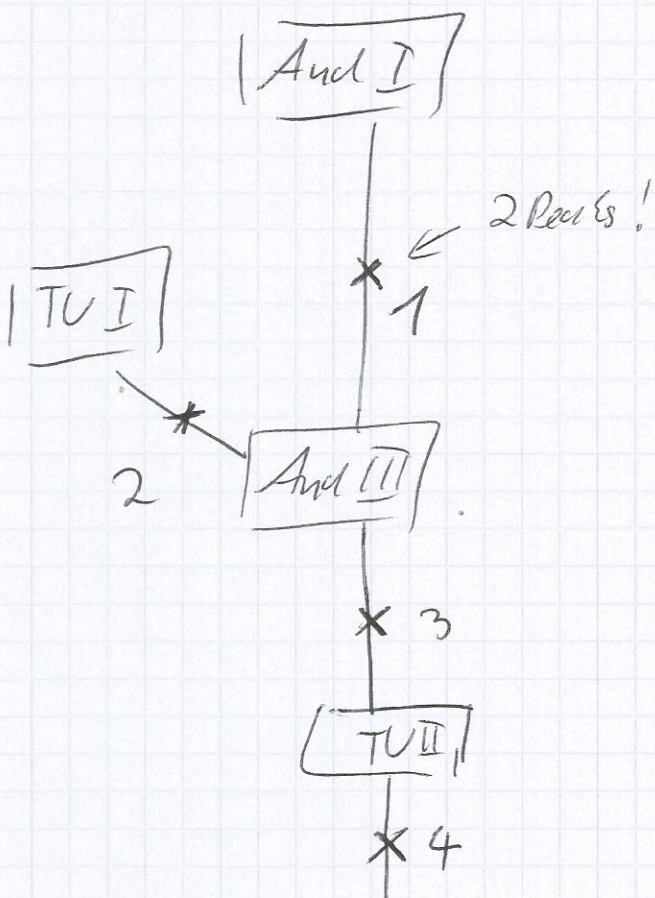
MR'

25/05/15

9



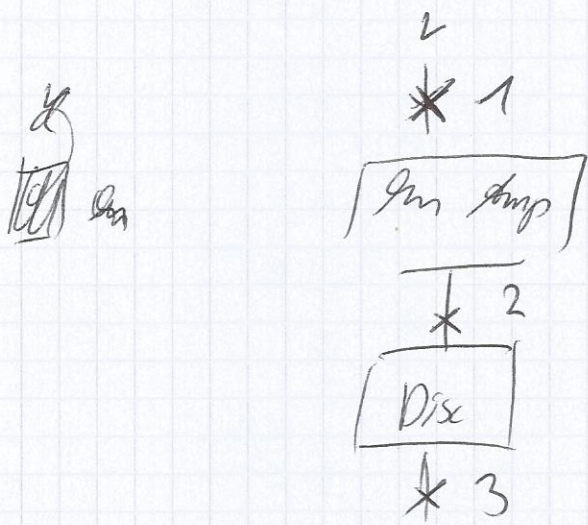
10

Tutor's sign

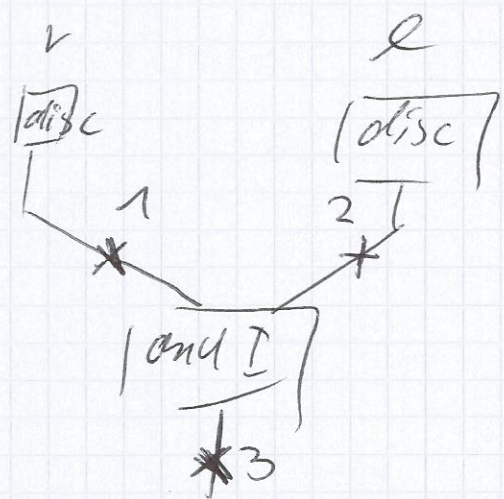
D R

25/03/15

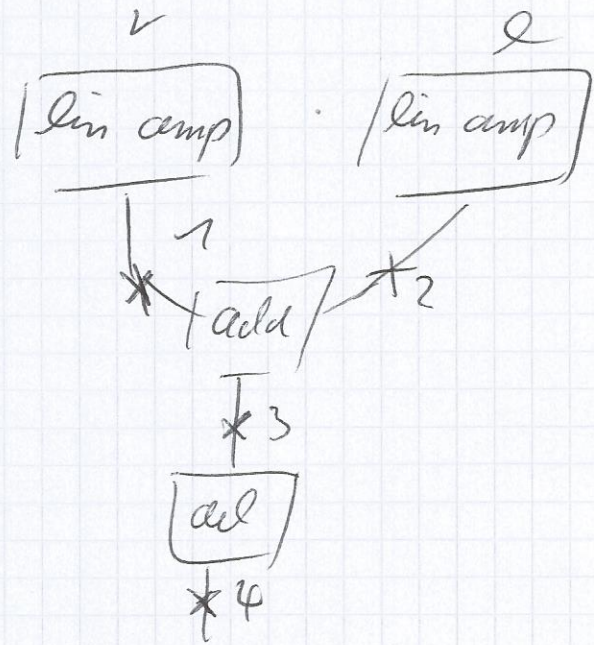
11



12



13

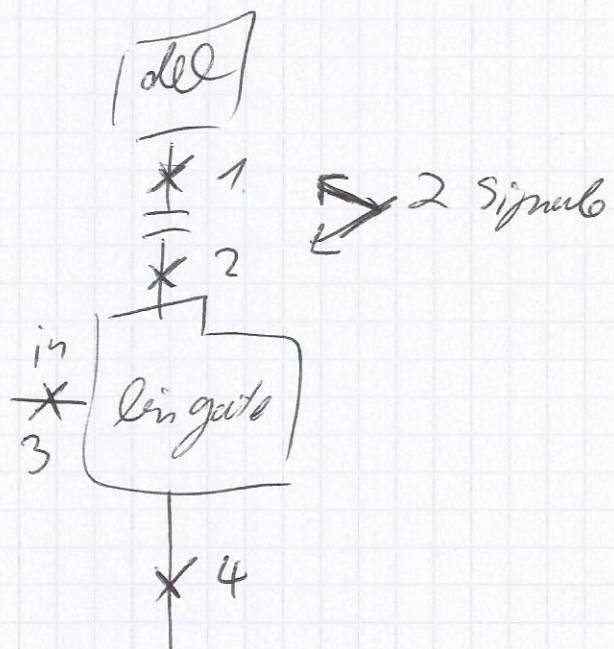


Tutor's sign

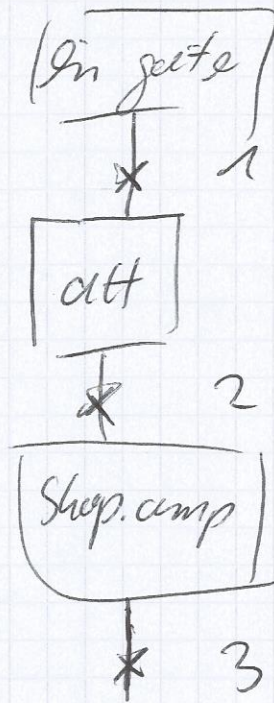
□ □

25/04/15

14



15



Über Kurkt:

Energieeichung 100%

$\hat{=}$  72 dB

Tintors dyn

$R_2 \cdot R'$   
25/05/15

Dose

5 m Pedestal

Pedestal minimiert  
mit Offset & Gauze

Any I

Any II

Any III

A B

A B C

A B C



Antwortwert: ~2,5 h

Photoelektronenstabilität:

Blitz

18% Pulseheight 1

LED-Dauer 2

für verschiedene Energien

sie 7-5 min

ch

Durchstrahl:

r

141 443 / 100s

e

788 65 / 100s

t

16 640 / 100s

b

17 181 / 100s



Blitze im Tank

r+t

106 649 / 1000s

t+b

108 / 100s

Einfly

t+r+t

20 990 / 1000s

Dunkelfly

t+b+r+t

973 / 1000s

2xjelle

213 / 1000s

Untergrund

116 / 1000s

Überlaufmessung

Dunkelflies 50%

(+ 6 dB)

Total 18dB

Total 13 hz

Ri

25/03/15

Freitag

Test  $\beta$ -v. Zeitmessung 60 min

3. Empfindlichkeit bei  $e^-$ -Peak (cG. 150)

Dämpfung: 21 dB

Übers WE: Hauptmessung

Montag

Bild Verformung Shaping Amp. 17/18

Kalibrierung	Dämpfung	Amp/mV
0 dB	19	<del>820</del> $840 \pm 40$
12 dB	20	<del>220</del> $210 \pm 10$
18 dB	21	$106 \pm 4$
27 dB	22	$75 \pm 4$

Tutor's Sign

DSR  
26/03/15

Zellblätter No, 274.

I: 10699

II: 2150

III: 20

/1000